System identification of the intrabrain tumoral uptake of multifunctional nanoparticles

Jean-Baptiste Tylcz, Denise Bechet, Thierry Bastogne, Hugues Garnier, Muriel Barberi-Heyob

▶ **To cite this version:**

HAL Id: hal-00753965

https://hal.archives-ouvertes.fr/hal-00753965

Submitted on 20 Nov 2012

System identification of the intrabrain tumoral uptake of multifunctional nanoparticles

Jean-Baptistie Tylcz [**] **Denise Bechet** [***] **Thierry Bastogne** [*]
Hugues Garnier [**] **Muriel Barberi-Heyob** [***]

*[*] INRIA-BIGS & Centre de Recherche en Automatique de Nancy
(CRAN), Université de Lorraine, CNRS UMR 7039, Campus Science,
BP 70239, 54506, Vandœuvre-lès-Nancy Cedex, France
[**] Centre de Recherche en Automatique de Nancy (CRAN), Université
de Lorraine, CNRS UMR 7039, Campus Science, BP 70239, 54506,
Vandœuvre-lès-Nancy Cedex, France
[***] Centre de Recherche en Automatique de Nancy (CRAN),
Université de Lorraine, CNRS UMR 7039, Centre Alexis Vautrin,
54511, Vandœuvre-lès-Nancy Cedex, France*

Abstract: Recent developments on multifunctional nano-systems have opened new perspectives for tumor control by proposing new nano-actuators and nano-sensors in *in vivo* anti-cancer treatments. But the delivery control of these nano-agents into the cancer cells is one of the major factors that directly affect the efficiency of nanotherapies. In this study, we show that system identification methods (CONTSID Matlab toolbox), generally used in control engineering, can bring efficient solutions to help biologists to estimate crucial parameters of the nanoparticles pharmacokinetics from experimental data. The *in vivo* results presented herein clearly emphasize the relevance of these data-driven modeling approaches associated with magnetic resonance imaging.

Keywords: System identification, pharmacokinetic model, biological system, nanotechnology, cancer

1. INTRODUCTION

In 2010, cancer has become one of the leading causes of death worldwide. Traditional anti-cancer therapies use standard treatment protocols, without accounting for existing variability between individuals or groups of population. That generally leads to a large uncontrolled inter-individual variability and a lack of predictability of therapeutic responses. Recent developments on multifunctional nano-systems have opened new perspectives for tumor control by proposing new nano-actuators and nano-sensors in *in vivo*[1] anti-cancer treatments (Allisona et al. (2008)). A direct consequence was the emergence of nanoparticle-based therapies such as the microwave hyperthermia therapy, thermoradiography, radioisotope therapy, charged-particle radiation therapy and the targeted photodynamic therapy (PDT). Photodynamic therapy is one of the noninvasive ways of treating malignant tumors. It relies on the selective uptake of a photosensitizing or radiosensitizing molecule (PS) in a tumor followed by exposure to the appropriate wavelength of light or X-ray to activate the photosensitizer. When activated by irradiation, the photosensitizer interacts with molecular oxygen to produce cytotoxic and short-lived species, such as singlet oxygen, that elicit both apoptotic and necrotic responses within treated tumors.

The delivery control of the photosensitising agent into the cancer cells is one of the major factors which directly affect the therapeutic efficiency of the photodynamic therapy (PDT) (Moser (1998); Bonnett (2000)). Many investigations have focused on the relationship between the molecular structure of PS and their extent of uptake by artificial membranes and cells. These have included porphyrins (Oenbrink et al. (1988)) and structurally related compounds, such as phtalocyanines (Margaron et al. (1996)), chlorines and pyropheophorbides (Henderson et al. (1997)). These studies concluded that the intracellular uptake could not be predicted from the chemical properties.

To better control the intratumoral uptake of the PS, recent studies have proposed to embed the photosensitizing agents into multifunctional nanoparticles (NP). Three recent scientific projects have provided new generations of photo- and radiosensitizers-doped nanoparticles. In the ANR EMED *Target-PDT* project[2], photosensitizers are encapsulated into lipid nanocarriers (Lipidots©) to treat head and neck cancers. In the ANR P2N *PDTX*[3] and INCA *Nano-Xrays* projects, scintillating nanoparticles are employed to combine radiotherapy and PDT for the treatment of brain tumors. Preliminary results of the ANR

---

[1] *i.e.,* within a living organism.

[2] ANR EMED *Target-PDT* (2010-2012)
[3] ANR P2N *PDTX* (2011-2013)

PCV *Nano-VTP* project [4] have clearly shown that a multifunctional nanoparticle technology can be adapted for imaging and treatment of brain tumors by interstitial PDT guided by MRI (Magnetic Resonance Imaging). Despite these promising results, the clinical development of multifunctional nanoparticles still requires a deeper insight into their *in vivo* pharmacokinetics.

The current knowledge about the uptake kinetics of PS into target cells is usually described by a few data points obtained during *in vitro* [5] kinetics experiments. However, this class of non-parametric models is not very well suited to the analysis, prediction and design of the PS uptake phase during PDT. The FDA's [6] 2004 Critical Path Report proposed, among other solutions, the increased use of model-based approaches to drug development, including pharmacokinetic and pharmacodynamic (PK/PD) modeling. The determination of a parametric model describing the uptake kinetics of photosensitising agents into living cells by extracting information from observations of input and output variables is a system identification problem (Ljung (1987); Walter and Pronzato (1997)). Several papers have been reported for the application of system identification techniques to pharmacokinetics modeling problems (Feng et al. (1996); Gomeni et al. (1988); Cobelli et al. (2000); Delforge et al. (2000); Sparacino et al. (2000); Audoly et al. (2001); Bastogne et al. (2007, 2008)). In particular, let us cite works of N. D. Evans et al. in (Evans et al. (2004, 2005)) in which a mathematical model for the *in vitro* kinetics of the anti-cancer agent topotecan is proposed. But till now, no system identification application has been devoted to the *in vivo* uptake pharmacokinetics of photosensitizers-doped nanoparticles (NP).

This study presents an *in vivo* application of a continuous-time systems identification method in a comparative study of pharmacokinetic characteristics for two different photosensitizers-doped nanoparticles used in the treatment of brain tumors. The model structure is derived from a compartmental modeling of the biological subject and the experimental data are extracted from MRI images analysis. The parameter estimation is performed by an algorithm of the CONTSID Matlab toolbox. Estimates of the model parameters for the two photosensitizers-doped nanoparticles are compared to analyze their *in vivo* pharmacokinetic properties such as their uptake and release rates from the brain tumor.

This paper is organized as follows. The biological system is presented in section 2. A modeling part is then described, with the continuous-time identification context in section 3. Estimation results are discussed in section 4 before drawing conclusions.

2. DESCRIPTION OF THE BIOMEDICAL PROCESS

Treatment of glioblastoma multiforme (GBM), a primary malignant tumor of the brain, is one of the most challenging problems. Surgery remains the basic treatment in which the bulk of the tumor is removed and the peripheral infiltrating part is the target of supplementary treatments.

Despite advances in neurosurgery, chemotherapy and radiotherapy the prognosis for patients with GBM, life expectancy at five years, is not higher than 10%. Gliomas treatment by radiotherapy requires high accuracy in delivering ionizing radiation to reduce toxicity to surrounding tissues. Since brain tissue is essentially transparent to light, it is a good environment for photodynamic therapy (PDT), which offers a localized treatment alternative in which improvements in local control of malignant cerebral gliomas may result in significant improved survival.

2.1 Material and methods

Animals and tumor model Male athymic nude rats (rnu-/rnu-) were used for this study (Harlan, Gannat, France). Rats (2-3/cage) were maintained in standard cages in isolators. Animals were housed with $12h$ light/dark cycle at 22-24°C and 50% humidity, and were administered with food and water ad libitum. The rats were used for tumor implantation at the age of 8 weeks (150-180g). Rats were anesthetized with a mixture of air and isoflurane concentrate (1.5-2% depending on the breathing) and placed into a Kopf stereotactic frame (900M Kopf Instruments, Tujunga, CA). Following antiseptic preparation of the head, a midline incision was done and a burr hole was drilled $0.5mm$ anterior and $2.7mm$ lateral to the bregma. A sterile needle ($150\mu m$ diameter) was slowly inserted $4.4mm$ into the brain parenchyma. 5.104 U87 cells were suspended in $5\mu L$ HBSS (1X) and were injected during 10 minutes with a flow of $0.2\mu L/min$ using a $10\mu L$ Hamilton syringe. After injection the burr hole was closed with bone wax, the scalp incision sutured (Suture 6.0 filament) and the surface was antiseptically cleaned.

Nanoparticles preparation for in vivo studies Nanoparticles were suspended in ultrapure water and NaCl 9‰(50:50) to obtain an equivalent concentration of $2.5mM$ TPC (photosensitizer) or $200mM$ Gd.Each batch of nanoparticles was buffered in order to obtain an iso-osmolar solution and pH 7.4 and conserved at $5°C$. Injected TPC amounted to 1.75 $\mu mol/kg$ and the injection solution was prepared by dissolution in 9‰NaCl to obtain an injection volume of $600\mu L$ (e.g. $0.437\mu mol$ of TPC or $84.2\mu mol$ of Gd for a body weight of $250g$). The anesthetized animal was catheterized into the caudal vein using a microperfusor (Microflex PVC: 0.4 mm/27 G, Vycon, Ecouen, France). The catheter was filled beforehand with 10% heparin (Heparin 25000 UI), which made it possible to check the venous return, the permeability of the catheter and to avoid its thrombosis by coagulated blood. $600\mu L$ of the NPs solution, following by $600\mu L$ of 9‰NaCl in order to rinse the extension set were injected during 1 minute.

Nanoparticles biodistribution The MRI experiments were performed at 7 Tesla in a horizontal bore magnet (Bruker, Biospec, Ettlingen, Germany). During acquisition the animal was anesthetized with a mixture of air and isoflurane concentrate (1.5-2% depending on the breathing). The rat head was fixed with ear plugs and bar tooth to prevent head movement during acquisition. The rat body temperature was maintained at $37°C$ using warm water circulating inside the bed. Animal breathing was monitored with a sensor pillow placed on the abdomen.

---

[4] ANR PCV *Nano-VTP* (2009-2011)
[5] *i.e.,* within a test tube or petri dish.
[6] U.S. Food and Drug Administration

Reference images (Scout views) were realized first to obtain the brain position inside the magnet. 15 slices were obtained, 5 in each plan (coronal, horizontal and sagittal). These slices allowed the positioning of the slices of the interest sequence. For the cerebral imaging, a volume coil (internal diameter 72 mm) was used for radio frequency emission, and a surface coil was placed on the animal skull for the reception of the signal. T2 weighted images coronal and horizontal T2 TurboRARE3 (Rapid Acquisition with Relaxation Enhancement) spin echo sequence were performed to know the position and the size of the tumor. The parameters of the sequences were: TR (Repetition Time)/TE (Echo Time) = 5000 / 77ms, matrix size 256 x 256 pixels, field of view (FOV), 40 x 40mm. For coronal images, 18 slices of 0.5mm without an intersection gap, and 20 slices of 0.85mm for axial images were acquired. The acquisition time for each sequence was 5.20 minutes. T1 weighted images axial and coronal T1 TurboRARE spin echo sequences were performed before and after the nanoparticles injection. The parameters were: TR/TE = 400/9 ms, matrix size 256 x 256 pixels, FOV, 40 x 40mm, Slice geometry was the same as the T2 weighted images. Time acquisition of each T1 weighted sequence was 2.30 min. Dynamic T1 weighted images were realized during the injection of the nanoparticles for characterization of the kinetics of the product inside the tumor. This sequence was a FLASH 4 (Fast Low-Angle SHot) sequence, which was set to obtain a temporal resolution of one image per 19 seconds. The parameters were: TR/TE = 200 /2.4ms, matrix size of 128 x 128 pixels, a 40mm square FOV. The kinetics was studied during one hour on an axial slice positioned at the level of the glioma.

3. DATA-BASED CONTINUOUS-TIME MODELING

Mathematical models of dynamic systems are required in most areas of scientific enquiry and take various forms, such as differential equations, difference equations, state-space equations and transfer functions. The most widely used approach to mathematical modeling involves the construction of mathematical equations based on physical laws that are known to govern the behavior of the system. If sufficient experimental or operational data are available, an alternative to physically-based mathematical modeling is data-based system identification (data-driven modeling), which can be applied to virtually any system and typically yields relatively simple models that can well describe the system's behaviour within a defined operational regime. Such models can be either in a black-box form, which describes only the input-output behavior, or in some other, internally descriptive form, such as state-space equations, that can be interpreted in physically meaningful terms. This section recalls some recent developments in system identification applied to the modeling of continuous-time systems from sampled data Garnier and Wang (2008).

3.1 Compartmental modeling

In this part, a compartmental modeling of the biological system is performed to characterize the model structure before starting the identification phase. The compartmental model is presented in Figure 1. The associated state-
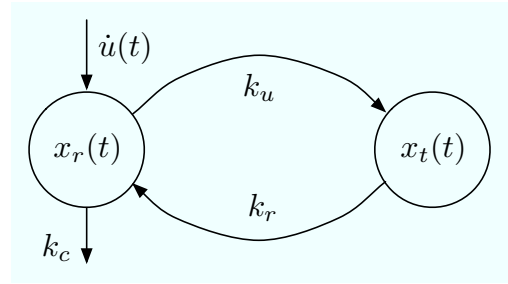

Fig. 1. Two-compartments model

space model is given by:
$$\begin{cases} \dot{x}_r(t) = \dot{u}(t) - k_c x_r(t) - k_u x_r(t) + k_r x_t(t) \\ \dot{x}_t(t) = k_u x_r(t) - k_r x_t(t) \\ y(t) = x_t(t) + e(t) \end{cases} \quad (1)$$
with
$$x_r(0) = x_t(0) = 0 \quad (2)$$
where $x_r(t)$ and $x_t(t)$ denote the amount of NP into the rat blood(first compartment) and into the brain tumor (second compartment) respectively. Parameters k_c, k_u, k_r are constant rates associated with the clearance, uptake and release of NP.
$$e(t) \overset{i.i.d.}{\sim} \mathcal{N}(0, \sigma^2) \quad (3)$$
is the output error. Model (1) finally leads to the following transfer function:
$$y(t) = \frac{k_u p}{p^2 + k_{ur} p + k_{rc}} u(t) + e(t), \quad (4)$$
with $k_{ur} = k_u + k_r$ and $k_{rc} = k_r k_c$. p is the differential operator, i.e. $p \cdot x(t) = \frac{dx(t)}{dt}$. The model structure defined in (4) is used in the identification phase (see subsection 3.6) to select the suited values for the structural indices of the transfer function. Estimates of k_u and k_{rc} are used as numeric criteria for comparing different nanoparticles with respect to their uptake and release pharmacokinetic characteristics, see section 3.7.

3.2 Problem formulation

Consider a linear, single-input, single-output, CT (Continuous Time) system whose input $u(t)$ and output $y(t)$ are related by a constant coefficient differential equation of order n
$$x^{(n)}(t) + a_1 x^{(n-1)}(t) + \ldots + a_n x^{(0)}(t) =$$
$$b_0 u^{(m)}(t) + b_1 u^{(m-1)}(t) + \ldots + b_m u^{(0)}(t) \quad (5)$$
where $x^{(i)}(t)$ denotes the ith time-derivative of the continuous-time signal $x(t)$. Equation (5) can also be written in the transfer function (TF) form:
$$x(t) = \frac{B(p)}{A(p)} u(t), \quad (6)$$
with
$$B(p) = b_0 p^m + b_1 p^{m-1} + \cdots + b_m,$$
$$A(p) = p^n + a_1 p^{n-1} + \cdots + a_n,$$
where p is the differential operator, i.e. $px(t) = \frac{dx(t)}{dt}$. It is assumed that the input signal $\{u(t), t_1 < t < t_N\}$ is applied to the system and that the output $x(t)$ is sampled at discrete times $t_1, \cdots, t_N$, not necessarily uniformly spaced. The sampled signals are denoted by $\{u(t_k); x(t_k)\}$.

In order to obtain high quality estimation results, it is vital to also consider the inevitable errors that will affect the measured output signal. The measured output $y(t_k)$ is assumed here to be corrupted by an additive discrete-time measurement noise $v(t_k)$

$$y(t_k) = x(t_k) + v(t_k).$$

The identification problem can now be stated as follows: estimate the parameters of the differential equation model from N sampled measurements of the input and output $Z^N = \{u(t_k); y(t_k)\}_{k=1}^N$.

Various statistical methods have been proposed to solve the parameter estimation problem outlined above and these have been formulated in both the time and frequency domains. However, only estimation in the time domain will be considered here, and only one direct estimation method will be considered: the Simplified Refined Instrumental Variable method for Continuous-time Systems (SRIVC). The SRIVC method is the only time domain method that can be interpreted in optimal statistical terms, so providing an estimate of the parametric error covariance matrix and, therefore, estimates of the confidence bounds on the parameter estimates.

3.3 The iterative SRIVC method

This approach involves a method of adaptive prefiltering based on a quasi-optimal statistical solution to the problem when the additive noise $v(t_k)$ is white.
Following the usual Prediction Error Minimization (PEM) approach (Maximum Likelihood (ML) in the present situation because of the Gaussian assumptions), a suitable error function $\varepsilon(t)$ is given by the output error (OE),

$$\varepsilon(t) = y(t) - \frac{B(p)}{A(p)} u(t).$$

Minimization of a least squares criterion function in $\varepsilon(t)$, measured at the sampling instants provides the basis for the *output error* estimation methods. However $\varepsilon(t)$ can also be rewritten as

$$\varepsilon(t) = \frac{1}{A(p)} \big(A(p)y(t) - B(p)u(t)\big).$$

Since the operators commute in this linear case, the filter $F(p) = 1/A(p)$ can be taken inside the brackets to yield

$$\varepsilon(t) = A(p)y_f(t) - B(p)u_f(t) \tag{7}$$

or,

$$\varepsilon(t) = y_f^{(n)}(t) + a_{n-1}y_f^{(n-1)}(t) + \ldots + a_0 y_f^{(0)}(t)$$
$$- b_m u_f^{(m)}(t) - \ldots - b_0 u_f^{(0)}(t) \tag{8}$$

where

$$\begin{cases} y_f^{(i)}(t) = f_i(t) * y(t), & i = 0, \ldots, n \\ u_f^{(i)}(t) = f_i(t) * u(t), & i = 0, \ldots, m, \end{cases} \tag{9}$$

and the set of filters now takes the form

$$F_i(p) = \frac{p^i}{A(p)}. \tag{10}$$

The associated estimation model can be written at time-instant $t = t_k$ in the form:

$$y_f^{(n)}(t_k) = \phi_f^T(t_k)\theta + \varepsilon(t_k) \tag{11}$$

where $\phi_f^T(t_k)$ and θ are defined as follow:

$$\phi_f^T(t_k) = \left[-y_f^{(n-1)}(t_k) \cdots - y_f^{(0)}(t_k) \, u_f^{(m)}(t_k) \cdots u_f^{(0)}(t_k) \right],$$
$$\tag{12}$$

$$\theta = [a_{n-1} \, \ldots \, a_0 \, b_m \, \ldots \, b_0]^T. \tag{13}$$

Thus, provided we assume that $A(p)$ is known, the estimation model (11) forms a basis for the definition of a likelihood function and ML estimation.

There are two problems with this formulation. The obvious one is, of course, that $A(p)$ is not known *a priori*. The less obvious one is that, in practical applications, we cannot assume that the noise $v(t_k)$ will have the nice white noise properties assumed above: it is likely that the noise will be a colored noise process, say $\xi(t_k)$. Both of these problems can be solved by employing a 'relaxation' optimization procedure that adaptively adjusts an initial estimate $A(p, \hat{\theta}^0)$ of $A(p, \hat{\theta}^j)$ iteratively until it converges on an optimal estimate of $A(p)$. And the colored noise problem is solved conveniently by exploiting IV estimation within this iterative optimization algorithm.

Of course, if the noise $v(t_k) = \xi(t_k)$ is colored, then the method is not quasi-optimal in statistical terms. However, experience has shown that it is robust and normally yields estimates with reasonable statistical efficiency (i.e. low but not minimum variance). However, albeit at the cost of increased complexity, it is possible to use a hybrid approach in the colored noise case, where the noise modeling, as well as the noise-derived parts of the prefiltering, are carried out in discrete-time terms (Garnier et al. (2008)).

3.4 Software

CONTSID toolbox: The CONtinuous-Time System IDentification (CONTSID) toolbox contains most of the parametric modeling methods developed over the last thirty years which allow one to directly identify CT models of linear time-invariant SISO, MISO and MIMO systems from uniformly and non-uniformly sampled data. It comprises most of the parametric estimation methods developed over the last thirty years, included the SRIVC technique outlined above. The toolbox is designed as an add-on to the Mathwork's System IDentification (SID) toolbox and has been given a similar setup. It can be downloaded from: *http://www.cran.uhp-nancy.fr/contsid/.*

3.5 Data processing

The response variable to be modeled corresponds to the mean value of the pixel intensities in a given region of interest associated with the brain tumor. This region of interest was selected by a segmentation process applied to MRI images whose an example is given in Figure 2. Each assay was repeated twice, on two different rats. The input variable (amount of NP administrated at time $t = 0$) is approached by a step signal.

3.6 Identification method

srivc algorithm from the CONTSID toolbox was used to estimate the parameters of the model (4). This model
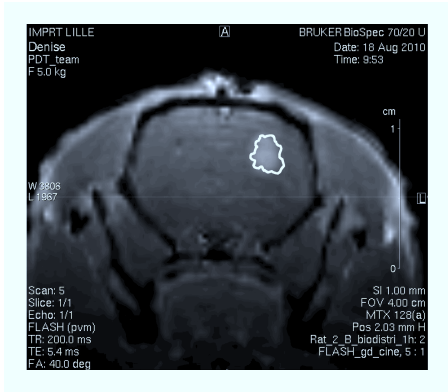
Fig. 2. Segmentation of the brain tumor from MRI images, the region of interest is enclosed by a white line.

structure has a pure derivative term on the numerator. Since *srivc* doesn't handle model with null parameter b_m (no *a priori* knowledge introduction), we have chosen to consider to use $Y(t) = \frac{y(t)}{p}$ (time integration of the measured response) as output variable instead of $y(t)$ initially. As a consequence, the model structure used in the identification procedure is now:

$$Y(t) = \frac{y(t)}{p} = \frac{k_u}{p^2 + k_{ur}p + k_{rc}} u(t) + v(t) \qquad (14)$$

with: $v(t) = e(t)/p$. Both $Y(t)$ and $u(t)$ were used for running the identification algorithm set up with parameters from table 1.

Table 1. *srivc* parameters

Parameters	Values
Output signal	$Y(t)$
Input signal	$u(t)$
Number of parameters in $A(p)$	2
Number of parameters in $B(p)$	1
Delay	0

3.7 Estimation results

The measured and simulated model outputs are compared in Fig. 3 to 6 (where the unit a.u. stands for arbitrary unit). For each rat, the mean intensity tumor selectivity of gadolinium oxide nanoparticles has been measured from total or peripheral regions of interest (ROI). One can observe that the model outputs fit quite well the measurement. However, the curves show that the model is slightly less effective for B series data. This is supposedly du to the difficulty to estimate of two very distant time constants, in our case one very fast (uptake phase), and the other really slow (release and clearance phase). The estimated parameters are presented in table 2.

4. DISCUSSION

Estimation results firstly show that the parameter k_u is larger for rats 3A and 6A (nanoparticle NP-TPC-ATWLPPR) than for rats 2B and 3B (NP-TPC). It means that the uptake kinetics with NP-TPC-ATWLPPR is slower than NP-TPC. We do not observe significant

Table 2. Estimated parameters

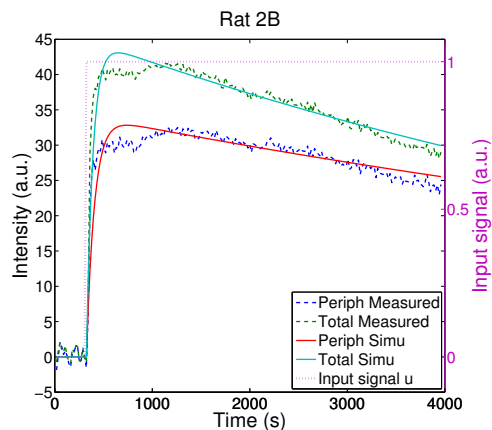| Rats	ROI	Estimates		
		k_u	k_{ur}	k_{rc}
3A	Total	39.57	5.81×10^{-3}	1.02×10^{-6}
3A	Peripheral	77.65	8.85×10^{-3}	2.11×10^{-6}
6A	Total	84.70	14.87×10^{-3}	4.33×10^{-6}
6A	Peripheral	166.73	24.68×10^{-3}	8.12×10^{-6}
3B	Total	0.34	11.49×10^{-3}	1.10×10^{-7}
3B	Peripheral	1.50	29.29×10^{-3}	2.38×10^{-6}
2B	Total	0.41	12.22×10^{-3}	9.71×10^{-7}
2B	Peripheral	0.68	15.34×10^{-3}	1.71×10^{-6}

Fig. 3. MRI signal intensity curves of nanoparticles NP-TPC (animal 2B) and their estimates
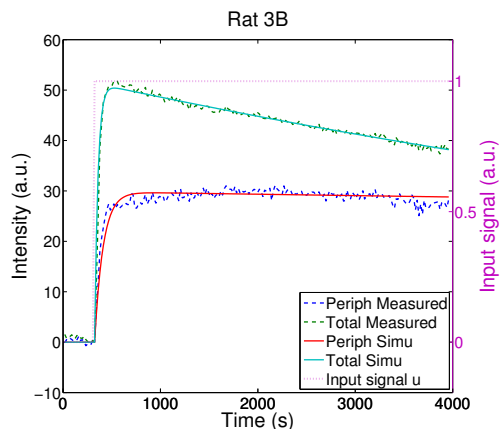

Fig. 4. MRI signal intensity curves of nanoparticles NP-TPC (animal 3B) and their estimates

differences for k_{ur}. Since $k_{ur} = k_u + k_r$, this result implies that k_r is larger for NP-TPC than for NP-TPC-ATWLPPR, *i.e.* a NP-TPC release kinetics slower than NP-TPC-ATWLPPR. These results are associated to two different fixing abilities and to the Enhanced Permeability and Retention (EPR) effect (which is the property by which certain sizes of nanoparticles tend to accumulate in tumor tissue) for the two nanoparticles. Even more interesting, estimated values of k_u are more important in peripheral regions. This result emphasizes that nanoparticles NP-TPC and NP-TPC-ATWLPPR mainly fix on the peripheral regions of the brain tumors. Parameter k_{rc} involves the NP blood clearance and diffusion in the interstitium phenomena (k_c). According to the estimates,
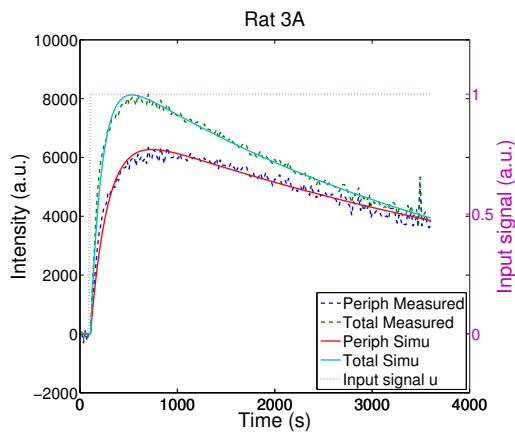
Fig. 5. MRI signal intensity curves of nanoparticles NP-TPC-ATWLPPR (animal 3A) and their estimates
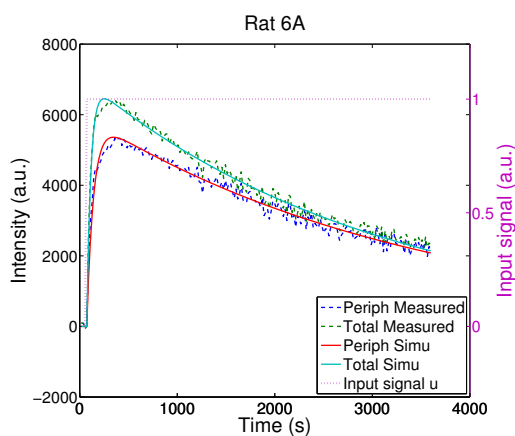

Fig. 6. MRI signal intensity curves of nanoparticles NP-TPC-ATWLPPR (animal 6A) and their estimates

one can conclude that it is faster with NP-TPC than NP-TPC-ATWLPPR.

5. CONCLUSIONS AND PERSPECTIVES

This study emphases the interest of system identification to the experimental modeling of *in vivo* uptake and release kinetics of nanoparticles in rats brain tumors. The experiment was carried out with two different nanoparticle batchs. The implemented data-driven modeling approach was based on a basic compartmental model structure and a continuous-time system identification algorithm (SRIVC, CONTSID Matlab toolbox). The *in vivo* data was derived from MRI images analysis. It is finally shown that one of the two tested nanoparticles have a real ability to fix in the peripheral of tumors. Further experiments should be performed to better understand now the bio-distribution kinetics of the nanoparticles in healthy organs such skin, muscle, kidney and liver.

ACKNOWLEDGMENT

REFERENCES

Allisona, R.R., Motaa, H.C., Bagnatob, V.S., and Sibata, C.H. (2008). Bio-nanotechnology and photodynamic therapy – state of the art review. *Photodiagnosis and Photodynamic Therapy*, 5, 19–28.

Audoly, S., Bellu, G., D'Angio, L., Saccomani, M., and Cobelli, C. (2001). Global identifiability of nonlinear models of biological systems. *IEEE Trans. Biomed. Eng.*, 48, 55–65.

Bastogne, T., Mézières-Wantz, S., Ramdani, N., Vallois, P., Tirand, L., Bechet, D., and Barberi-Heyob, M. (2008). Parameter estimation of pharmacokinetics models in the presence of random timing errors. *European Journal of Control*, 14(2).

Bastogne, T., Tirand, L., Bechet, D., Barberi-Heyob, M., and Richard, A. (2007). System identification of photosensitiser uptake kinetics in photodynamic therapy. *Biomedical Signal Processing and Control*, 2, 217–225.

Bonnett, R. (2000). *Chemical Aspects of Photodynamic Therapy*. Gordon and Breach Science Publishers.

Cobelli, C., Toffolo, G., and Foster, D. (2000). *Tracer Kinetics in Biomedical Research: From Data to Model*. Kluwer Academic Publishers.

Delforge, J., Sirota, A., and Mazoyer, M.B. (2000). Identifiability analysis and parameter identificaion of an *in vivo* ligand-receptor model from PET data. *IEEE Trans. Biomed. Eng.*, 37(7), 653–661.

Evans, N.D., Errington, R.J., Chapman, M.J., Smith, P.J., Chappell, M.J., and Godfrey, K.R. (2005). Compartmental modelling of the uptake kinetics of the anti-cancer agent topotecan in human breast cancer cells. *International Journal of Adaptive Control and Signal Processing*, 19, 395–417.

Evans, N.D., Errington, R.J., Shelley, M., Feeney, G.P., Chapman, M.J., Godfrey, K.R., Smith, P.J., and Chappell, M.J. (2004). A mathematical model for the *in vitro* kinetics of the anti-cancer agent topotecan. *Mathematical Biosciences*, 189, 185–217.

Feng, D., Huang, S.C., Wang, Z., and Ho, D. (1996). An unbiased parametric imaging algorithm for non-uniformly sampled biomedical system parameter estimation. *IEEE Transactions on Medical Imaging*, 15(4), 512–518.

Garnier, H. and Wang, L. (eds.) (2008). *Identification of continuous-time models from sampled data*. Springer-Verlag, London.

Garnier, H., Gilson, M., Bastogne, T., and Mensler, M. (2008). The CONTSID Toolbox: a Software Support for Data-based Continuous-time Modelling. In *Identification of continuous-time models from sampled data*, 249–190. Springer-Verlag. URL http://hal.archives-ouvertes.fr/hal-00161980.

Gomeni, R., Piet-Lahanier, H., and Walter, E. (1988). Study of the pharmacokinetics of betaxolol using membership set estimation. *Biomed. Meas. Infor. Contr.*, 2(4), 207–211.

Henderson, B.W., DA, D.A.B., Greco, W.R., Sharma, R.K., Pandey, R.K., L. A. Vaughan, K.R.W., and Dougherty., T.J. (1997). An *in vivo* quantitative structure-activity relationship for a congeneric series of pyropheophorbide derivatives as photosensitizers for photodynamic therapy. *Cancer Research*, 57, 4000–4007.

Ljung, L. (1987). *System Identification: Theory For The User*. Prentice Hall, Englewood Cliffs, NJ.

Margaron, P., M.-J. Grégoire, V. Scasnar, H.A., and van Lier, J.E. (1996). Structure-photodynamic activity relationships of a series of substituted zinc phthalocyanines. *Photochem. Photobiol.*, 63, 217–223.

Moser, J.G. (1998). *Photodynamic Tumor Therapy: 2nd and 3rd Generation*. Gordon & Breach Science Publishers.

Oenbrink, G., Jurgenlimke, P., and Gabel, D. (1988). Accumulation of porphyrins in cells: influence of hydrophobicity aggregation and protein binding. *Photochem. Photobiol.*, 48, 451–456.

Sparacino, G., Tombolato, C., and Cobelli, C. (2000). Maximum-likelihood versus maximum a posteriori parameter estimation of physiological system models: the C-peptide impulse response case study. *IEEE Trans. Biomed. Eng.*, 47(6), 801–811.

Walter, E. and Pronzato, L. (1997). *Identification of Parametric Models from experimental data*. Springer-Verlag, Masson.